Vol. 514: 119–135, 2014
doi: 10.3354/meps10977

MARINE ECOLOGY PROGRESS SERIES
Mar Ecol Prog Ser

Published November 6

Transport and retention of vertically migrating adult mysid and decapod shrimp in the tidal front on Georges Bank

R. Gregory Lough[1,*], Alfredo Aretxabaleta[2,3]

[1]Northeast Fisheries Science Center, NMFS, NOAA, Woods Hole, MA 02543, USA
[2]Coastal and Marine Science Center, USGS, Woods Hole, MA 02543, USA
[3]Integrated Statistics, Woods Hole, MA 02543, USA

ABSTRACT: Vertical profiles of the adult epibenthic shrimp *Neomysis americana* and *Crangon septemspinosus* obtained during June 1985 were used to simulate possible rates of ascent from bottom (40 to 50 m) to near surface at night and return by day, and the consequence of these rates on their horizontal distribution. Numerical particles were released at the sampling site using archived model current fields with specified vertical rates (from no swim behavior to 20 mm s^{-1}) and tracked for up to 30 d. The best match between observed and modeled vertical profiles was with a vertical swimming speed of 10 mm s^{-1} for *N. americana* and 2 mm s^{-1} for *C. septemspinosus*. Whereas *N. americana* rapidly swims towards the surface at dusk and descends to bottom by dawn, *C. septemspinosus* tends to only swim up to the middle of the water column at night. After 16 d, the simulation with 10 mm s^{-1} swim speed showed most particles were concentrated in an area centered around the 60 m isobath, where the tidal front was located. At 2 mm s^{-1} swim speed particles were concentrated more shoalward onto the western end of Georges Bank. *N. americana* are expected to be more closely associated with the tidal front, since they spend more time near the front surface convergence, but are more likely to be transported off the bank due to the southwestward-flowing surface tidal jet, whereas *C. septemspinosus* would be retained primarily on the bank, since they are found deeper in the water column during both day and night.

KEY WORDS: *Neomysis* · *Crangon* · Vertical distribution · Migration · Tidal front · Georges Bank

INTRODUCTION

Mysids are an important part of the mobile benthic epifauna of mid-latitude continental shelves and a major dietary component for many fish and invertebrates (Jumars 2007). The decapod shrimp *Crangon septemspinosus*, sand or brown shrimp, is also an important part of the benthic epifauna on continental shelves and as prey for demersal fishes around the North Atlantic. *Neomysis americana*, opossum shrimp, is the most abundant mysid in the coastal waters of the United States between Virginia and New England (Wigley & Burns 1971, Williams et al. 1974). Link & Garrison (2002) found mysids in 80% of gut contents of juvenile cod <10 cm on the New England Shelf. Georges Bank has the highest density and biomass of mysids; these are most abundant in shallower areas, preferring sand sediment for feeding (Whiteley 1948, Theroux & Wigley 1998). They can be found from the intertidal zone to 90 m depth but are most abundant between 30 and 60 m (Wigley & Burns 1971) (Fig. 1). Mysids are omnivorous and can be an important predator on zooplankton (Fulton 1982). Field studies of gut contents of mysids indicated detritus feeding during the day but more zooplankton feeding during the night.

Two major spawnings occur, one in spring (March through June) and another in late summer and fall

*Corresponding author: gregory.lough@noaa.gov

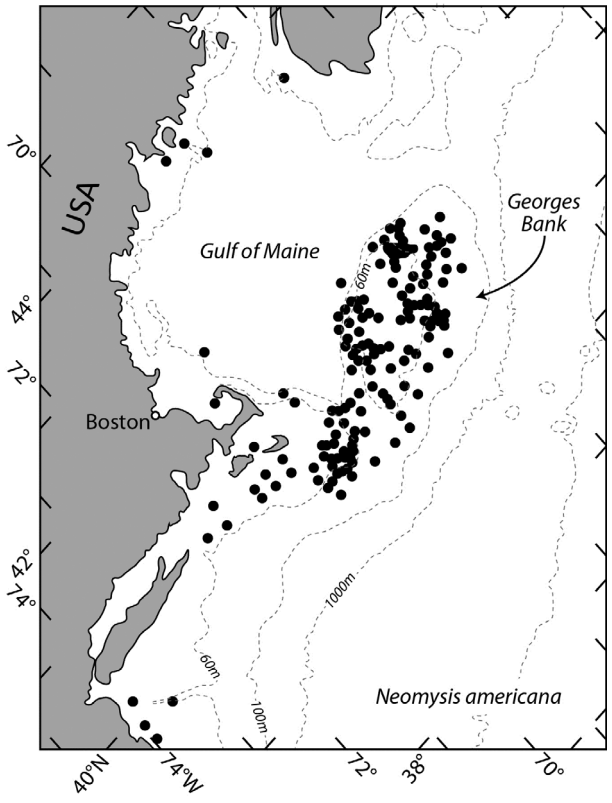

Fig. 1. *Neomysis americana* benthic sample distribution (●) redrawn from Wigley & Burns (1971)

(August through October) (Wigley & Burns 1971). The highest abundance of spawning adults from the spring generation centers on June/July, and from the fall generation, on the following April/May. Adults from the summer generation are smaller (6 to 10 mm) than those from the winter generation (10 to 15 mm). The eggs and larvae develop in adult female brood pouches and are liberated into the plankton as juveniles at 4 to 5 mm in length. This mysid is eurythermic, but reproduction is affected by the temperature regime, the sequence, timing, or duration of which may be important (Wigley & Burns 1971). Furthermore, mysids are gregarious and may only live a year.

N. americana has been observed to undergo a regular pattern of diel vertical migration, primarily controlled by light intensity, moving off the bottom towards the surface by night and returning to the bottom by day (Herman 1963, Mauchline 1980, Abello et al. 2005). Young mysids are generally higher up the water column than adults. Immature mysids undergo migrations throughout most of the year; mature individuals only migrate during the spawning season, and copulation may only occur at night and be correlated with molting females. Diel behavior varies due to shorter days in spring and fall. Abello et al. (2005) further indicated that emergence and reentry events of the mysid shrimp *N. americana* take place within 1 h of sunset and sunrise, respectively, at a site 10 m deep in the Damariscotta River estuary, Maine. Their mean ascent (0.29 ± 0.03 cm s^{-1} [±1 SE]) and descent (-0.26 ± 0.02 cm s^{-1}) velocities are fairly stable, indicating the cue is based on the relative rate of change in light intensity and not the progress of isolumes or absolute rate of change in light intensity. Taylor et al. (2005) found that the nocturnal emergence behavior of *N. americana* in the Damariscotta River estuary in Maine occurs 3.5 to 4.0 h after the first slack tide; this appears to be related to the emergence of benthic copepods and may explain the more limited numbers of daytime emergences. Sato & Jumars (2008) also found nocturnal emergence behavior in *N. americana* in the Damariscotta River estuary, but it appeared to be shifted in relation to the semidiurnal tidal period in the fall. *N. americana* reach the surface of the water column only during low slack tides and avoid the surface in periods when the fastest currents occur. Thus, cues for multiple emergence behaviors can be complex, and factors include light intensity, tidal currents, searching for prey, escape from predators, reproduction and circatidal rhythms.

On Georges Bank and in southern New England, *C. septemspinosus* are mostly found near the 100 m isobath and in sandy sediments (Whiteley 1948, Richards & Riley 1967, Theroux & Wigley 1998) (Fig. 2). While remaining burrowed within the sediments by day, they become active at dusk and can be found in the water column at night (Tiews 1970). Daily tidal migrations have also been observed (Hartsuyker 1966, Al-Adhub & Naylor 1975). They have an extended breeding season, and ovigerous females were found in spring and early summer, leading to possibly 1 brood yr^{-1} on Georges Bank (Whiteley 1948). In Long Island Sound, Richards & Riley (1967) found that the greatest percentage of ovigerous females occurs in June. Eggs hatch as larval planktonic zoea stages at 2 to 3 mm in length and develop to post-larvae/juveniles. They are considered juveniles at around 8 to 19 mm, and ovigerous females are found among individuals with lengths >20 mm (Richards & Riley 1967). *C. septemspinosus* are omnivorous (Price 1962), solitary and can live 2 to 3 yr.

Adults of both species appear to be associated with the tidal front on Georges Bank, perhaps because of their migratory behavior, which may enhance mating and feeding on the increased abundance of prey also accumulating at the front. If aggregation at the tidal front is important to population survival, then what

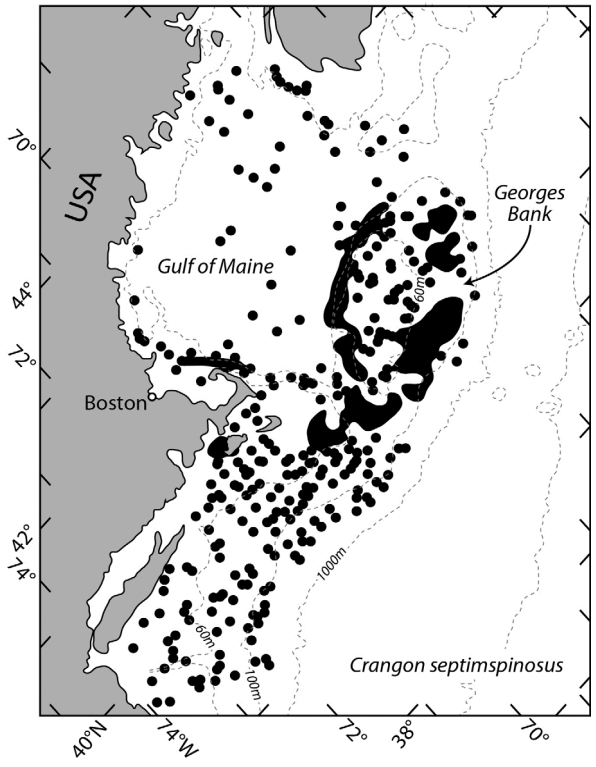

Fig. 2. *Crangon septemspinosus* benthic sample distribution (●) redrawn from Theroux & Wigley (1998). High density of samples result in overlapping dots

are the factors determining aggregation versus loss from the Bank?

A tidal front develops on Georges Bank in late spring along the 60 m isobath, separating the tidally well-mixed shoals from the deeper, thermally stratified water on the southern flank. The residual clockwise circulation around Georges Bank is primarily due to the topographic rectification of the tidal currents (Loder & Wright 1985). A strong tidal front 'jet' current is created near the maximum cross-bank density gradient flowing along-bank to the southwest on the southern flank. A secondary 2-cell circulation pattern can develop across-bank, with upwelling on the mixed and stratified sides of the front and downwelling in the vicinity of the front, resulting in a near-surface convergence and a near-bottom divergence. Fish larvae are transported along the southern flank in the spring when the tidal front is developing and appear to have continuous recruitment to the central shoal region of the Bank (Lough & Manning 2001). The importance of the front as a retention mechanism has been hindcast in 3-dimensional circulation models that provide evidence of the accumulation of particles when the cell-like circulation is active (Aretxabaleta et al. 2005, Lough et al. 2006a).

It is difficult to adequately assess the population distribution and abundance of these 2 species from field surveys due to marked differences in diel catchability of the migrating adults. Besides gear avoidance of smaller, slower nets, the adults remain on the bottom during the day, below the maximum sampling depth of midwater gear. Micro-nekton were sampled routinely during the Georges Bank U.S. GLOBEC monthly broadscale surveys from January to June, 1995 to 1999, using a 10 m^2 MOCNESS (multiple opening/closing net and environmental sensing system, 3 mm mesh) (Brown et al. 2005). The samples showed peak abundance of both *N. americana* and *C. septemspinosus* in the spring. Monthly April to June distribution plots showed the highest abundance to be around the 60 m isobath or around the seasonally developing tidal front which separates the shoal's well-mixed crest from the stratified southern flank. In May 1999, a very high concentration of both species occurred on the western side of Georges Bank. Brown et al. (2005) collected specimens of both species exclusively associated with Georges Bank/Gulf of Maine water, and their distributions did not appear to be affected by warm water intrusions during late spring/summer. They suggested that the species' bottom-seeking strategy may allow them to avoid displacement when flows become strong or when temperatures rise.

The European mysid *Neomysis integer* was found to be most abundant in low flow areas in estuaries, and laboratory experiments demonstrated that they respond to strong flow by seeking low flow regimes near the bottom (Lawrie et al. 1999, Speirs et al. 2002). Bottom-seeking behavior can result in position maintenance or behavioral adaptations, such as emerging into the water column during flood tide which can facilitate entry into an estuary, a process known as 'selective tidal stream transport' (Sato & Jumars 2008, Daewel et al. 2011). On Georges Bank the strong semidiurnal rotary currents are relatively uniform throughout the well-mixed, 60 m water column and would not appear to be the initiating factor for vertical behavior. The bottom boundary layer would provide the lowest flow habitat; so what is the primary controlling factor for the vertical migratory behavior of these species? These 2 shrimp species are endemic to Georges Bank, and their life cycles do not require transport into estuaries as nursery areas. Instead, it is important that they are retained on the shelf, where the bottom habitat is beneficial to feeding and survival. The seasonally developing tidal front on Georges Bank has been shown to be an important feature for the aggregation and retention

of planktonic organisms. The objective of this study was to characterize their observed vertical distribution and use particle-tracking simulations to determine how the tidal front influences their horizontal distribution and retention/loss off Georges Bank. The best available diel time-series of *N. americana* and *C. septemspinosus* were collected by the first author during a June 1985 survey on the southeastern side of Georges Bank, near the tidal front. Numerical experiments were carried out using a range of possible diel vertical migration behaviors to see which ones best matched the observed profiles before simulating the species' transport. The 2 species studied have different sizes and morphologies, which may influence their migratory behaviors. In a dorsal/ventral orientation *C. septemspinosus* is almost twice the size of *N. americana*, which shows a more lateral body compression. Their apparent migratory behaviors were compared and contrasted by simulation experiments.

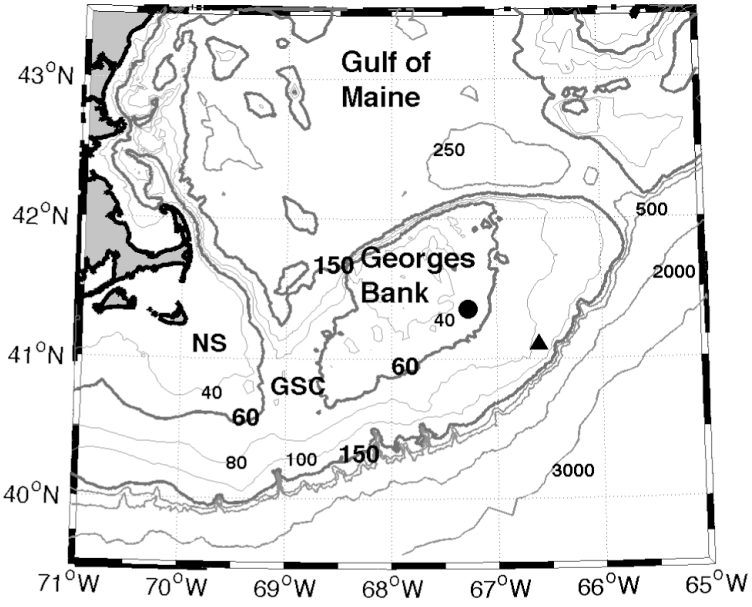

Fig. 3. Gulf of Maine/Georges Bank map showing location of sampling station (●) near the southeastern part of Georges Bank. (▲) NDBC (National Data Buoy Center) Buoy 44011. Depth contours are in meters. GSC: Great South Channel; NS: Nantucket Shoals

MATERIALS AND METHODS

Georges Bank study site and sampling strategy

The study site was located on the southeastern side of Georges Bank (Fig. 3) at 41°19'N, 67°19'W, between 40 and 50 m water depth and was chosen based on the high densities of young cod juveniles. A 10 m^2 MOCNESS (Wiebe et al. 1985) was used for a vertical time-series of 5 tows at this site from 17 to 19 June 1985, sampling the water column in 10 m strata, each net for 30 min (3.0 mm stretch mesh) at 4 depths (40–30, 30–20, 20–10 and 10–0 m; Table 1). Vessel speed during towing was 2 to 3 knots. The volume of water was monitored electronically, and on average 19 000 m^3 of water was filtered during a 30 min tow. Temperature and salinity data were taken from the attached conductivity-temperature-depth sensor, and composite water-column profiles were made. The hydrographic data were available for assimilation into general circulation simulations such as the hindcast product described in the following section. An EPSCO Chromoscope Fish Finder CVS-886 (at both 50 and 200 kHz) was deployed aboard the vessel to monitor scattering layers during sampling.

All invertebrates were removed from net samples or aliquots were taken; individuals were identified, measured and standardized regarding number of species or stages per 10 000 m^3 within a stratum. Body length was measured from the anterior margin of the carapace to the posterior end of the telson. Length frequencies of *Neomysis americana* and *Crangon septemspinosus* were plotted as a percent-

Table 1. Summary of 10 m^2 MOCNESS tows on the southeastern Georges Bank from 17 to 19 June 1985. Sampled strata for each tow were 40–30, 30–20, 20–10 and 10–0 m. EDT: Eastern Daylight Time

MOCNESS tow	Date	Time (h, EDT) Start / End	Bottom depth (m) Start / End	Latitude N, Longitude W Start / End
519	17 Jun 1985	23:49 / 01:59	47 / 44	41°18.7′, 67°18.8′ / 41°25.6′, 67°17.1′
521	18 Jun 1985	13:24 / 15:26	44 / 43	41°20.5′, 67°18.5′ / 41°27.7′, 67°16.4′
522	18 Jun 1985	19:51 / 21:52	48 / 48	41°19.2′, 67°14.0′ / 41°21.3′, 67°15.4′
523	19 Jun 1985	02:37 / 04:38	46 / 49	41°22.8′, 67°17.4′ / 41°19.9′, 67°13.4′
524	19 Jun 1985	09:35 / 11:36	49 / 47	41°21.0′, 67°14.4′ / 41°18.6′, 67°18.6′

age of the total number of each stage: male, female and ovigerous female. The 3 stages were identified to show the composition of the length–frequency catches, since it is possible that each stage may have a different migratory behavior.

Particle tracking using archived simulations

Archived modeled currents for 1985 were obtained from the Northeast Coastal Ocean Forecast System (NECOFS) 33 yr hindcast, which uses the finite volume coastal ocean model (FVCOM; Chen et al. 2003). The FVCOM is a prognostic, unstructured-grid, finite-volume, primitive equation circulation model, and the NECOFS implementation includes the entire Gulf of Maine with open-ocean boundaries along the New Jersey and Scotian shelves. Hourly values were downloaded from the hindcast archive (www.smast.umassd.edu:8080/thredds/dodsC/fvcom/hindcasts/30yr_gom3.html). The NECOFS implementation has 45 layers in the vertical and a horizontal resolution of around 3 km over Georges Bank. The NECOFS implementation uses a global tidal model to provide tidal forcing in the boundary and the mesoscale meteorological models WRF (Weather Research and Forecasting model) and MM5 (fifth-generation NCAR/Penn State non-hydrostatic mesoscale model) for atmospheric forcing (more details in http://fvcom.smast.umassd.edu/research_projects/NECOFS/).

In the present study, organisms were represented as particles in the 3-dimensional model current field. Particles were released uniformly below 40 m at the sample location over a circular area of 5 km^2 (to partially include sampling position uncertainty and be consistent with previous particle-tracking studies that characterized regional connectivity; Mitarai et al. 2009, Aretxabaleta et al. 2014, Li et al. 2014) centered on the sampling location for the period of sampling (17 to 19 June 1985). Particles were initialized uniformly every meter in a volume from 1 to 5 m from the bottom every hour before the first vertical ascent started. Particles were tracked in 5 min time steps, and the output was saved hourly. The numerical particle trajectories were calculated with an offline particle-tracking model (DROGUE3D: Blanton 1993) using the archived simulated FVCOM currents. Lagrangian tracking included a fourth-order Runge-Kutta scheme for advection. A reflective boundary condition was applied to prevent particles from exiting the horizontal edge of the domain or escaping through the bottom or surface. To provide representative results, a sufficient number of particles had to be used. In the current simulations a total of 120 000 particles were released in each experiment (4800 particles km^{-2}, i.e. a particle every 15 m, at each of the 5 depths).

The particles' turbulent behavior in the vertical was simulated by assuming uncorrelated random walk. The root-mean-squared (RMS) size of the random vertical displacement (R_z) over each time interval (Δt) was given by $R_z = \sqrt{2A_z\Delta t}$, where A_z is the vertical turbulent eddy viscosity taken from the model. The turbulent closure used in the FVCOM hindcast is the Mellor-Yamada 2.5 (Mellor & Yamada 1982), and the resulting eddy viscosities were obtained from the archive.

The turbulent behavior for the particles in the horizontal direction required an equivalent parameter to the vertical eddy viscosity but for the horizontal. Such a parameter was not provided in the archived model. The horizontal eddy diffusivity was approximated using the Smagorinsky (1963) formulation which depends on the resolved horizontal shear and the model grid scale. The resulting RMS of the random horizontal displacement (R_h) is $R_h = \sqrt{2A_h\Delta t}$, where A_h is the horizontal turbulent eddy diffusivity.

Particles followed the velocity field; however, they were not strictly passive, as they also migrated in the vertical according to varying vertical swimming speeds. The basic run included no vertical swimming behavior, but particles were still moved in the vertical by the model vertical velocity and the random turbulent displacement associated with vertical eddy viscosity. The tested swimming speeds were: 0.5, 1, 2, 5, 10 and 20 mm s^{-1}. Sensitivity to the timing of the vertical swimming velocities was investigated by modifying the time of the initialization and finalization of the upward/downward velocities around dusk/dawn (not shown), but the differences between timing scenarios were small and made the interpretation of the results more complex. The duration of vertical migration ranged from 1 to 3 h and stopped if the particles reached the surface or bottom boundary. The numerical particles released at the location of the MOCNESS observations were tracked for up to 30 d. Particles that crossed the 200 m isobath were considered lost from Georges Bank and were no longer tracked. Passive sinking was not included, since the rates of sinking are minimal (<0.5 mm s^{-1}, based on particles on the order of 10 to 25 mm, with fractal dimensions between 1.5 and 2; Winterwerp & van Kesteren 2004) when compared to the vertical migration speeds and random vertical displacements associated with turbulence.

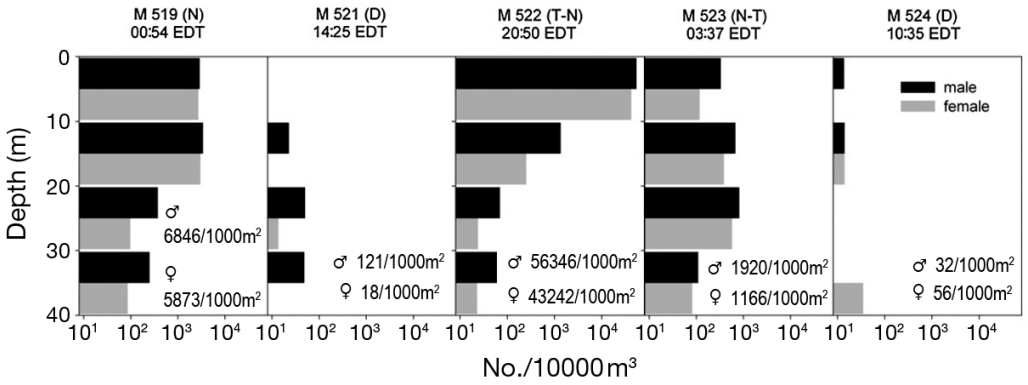

Fig. 4. Vertical distribution of *Neomysis americana* from five 10 m MOCNESS tows at a location on the southeastern Georges Bank from 17 to 19 June 1985. Water depths ranged from 43 to 49 m. The MOCNESS tow number and time mid-point are located above each column and designated as night (N), day (D), or twilight (T) in parentheses. EDT: Eastern Daylight Time. Male (black) and female (gray) densities are shown as separate bars within a 10 m stratum. Note the $\log_{10}$ density scale. Water column abundances (no./1000 m^2) of males and females are included below each tow panel

RESULTS

A marked return signal appeared on the EPSCO Chromoscope Fish Finder, forming near the surface soon after sunset (18:15 h Eastern Daylight Time [EDT]); then a layer about 10 m thick descended towards the bottom at sunrise (05:03 h). The signal finally disappeared from the scope by about 06:30 h each day. A population vertical migration rate from surface to bottom (87 min to 43–49 m) is estimated to be 8.2 to 9.4 mm s^{-1}. Based on the MOCNESS tow catches, the scattering layer observations were probably due to the dense aggregation of *Neomysis americana*.

MOCNESS observations

Mysids were the dominant invertebrates caught by the 10 m^2 MOCNESS in night tows on the southeastern side of Georges Bank from 17 to 19 June 1985. All 5 MOCNESS tows were carried out within a 36 h period, with bottom depths ranging from 43 to 49 m. The water column was well-mixed, with a temperature of 10.5°C (SD = 0.14) and salinity of 32.671 (SD = 0.061), with no apparent vertical structure. The observed vertical distribution of *N. americana* (Fig. 4) from MOCNESS tows showed males and females to be similar in abundance and vertical distribution. During the night (M 519) and twilight–night (M 522) tows, *N. americana* were distributed throughout the 40 m water column, with highest densities in the upper 20 m. During the night–twilight tow (M 523), they were distributed more evenly throughout the water column. *N. americana* were mostly absent during the 2 d tows (M 521, M 524), presumably because they were below a water depth of 40 m, where sampling was not possible. Length frequencies for the 3 stages were highest for the 14 to 16 mm size classes, which would indicate that shrimp were probably from the winter generation (Table 2, Fig. 5). A few individuals were caught in the 6–13 mm and 17–18 mm size classes. Only 13% of the females were ovigerous.

The observed vertical distribution of *Crangon septemspinosa* (Fig. 6) from MOCNESS tows showed males and females to be similar in abundance and vertical profiles, but their water column abundance was an order of magnitude lower than that of *N. americana*. During the night tow (M 519) and night–twilight tow (M 523) *C. septemspinosa* were distributed throughout the 40 m water column, although higher densities were located below 20 m. They were mostly absent during the 2 d tows (M 521,

Table 2. Mean lengths (mm) and standard deviations of *Neomysis americana* and *Crangon septemspinosus* life stages collected by the 10 m^2 MOCNESS in June 1985. Length–weight functions for all stages combined are also given, where W is wet weight (mg) and L is length (mm)

	n	Mean (1 SD)
N. americana		
Males	35481	14.81 (1.12)
Females	25400	14.71 (1.15)
Ovigerous	3333	15.01 (1.14)
$W = 0.223L^{2.5089}$, n = 164, r = 0.94, $r^2 = 0.89$		
C. septemspinosus		
Males	5265	24.42 (11.75)
Females	2201	24.30 (3.08)
Ovigerous	352	29.46 (1.47)
$W = 0.0014L^{3.3410}$, n = 88, r = 0.98, $r^2 = 0.96$		

M 524) and the twilight–night tow (M 522). Length frequencies for the 3 stages show ovigerous females to be larger (27–32 mm size class, mean 29.46 mm, SD = 1.47 mm) than the males and females (Table 2, Fig. 5). Mean lengths for males and females were about 24 mm and ranged from 15 to 33 mm. Only 16% of females were ovigerous.

Flow characterization

The archived model data were downloaded for the period June to July 1985, to match the period when the 17 to 19 June 1985 MOCNESS observations were collected. As the objective of the current study was to characterize normal conditions over Georges Bank, the June to July 1985 wind velocities and depth-averaged velocities were compared with average climatological values (Table 3). Wind velocity data from the National Data Buoy Center (NDBC) Buoy 44011 were averaged for all available years (1984 to 2012) and compared to the wind observed from June to July 1985. The observed June to July 1985 values were within 10% of the long-term average, suggesting the atmospheric forcing during 1985 was representative of average conditions.

Average water velocities were obtained from climatological model solutions provided by Naimie et al. (1994) and compared with the FVCOM archived depth-averaged velocities for 1985. The magnitude of the total velocities was dominated by tidal fluctuations, which have little interannual variability; therefore, the velocity magnitudes during 1985 were similar to the long-term values. When the depth-averaged subtidal (40 h low-pass filtered) velocities were considered, the magnitude of the velocities during 1985 in the east–west direction (U) was comparable to the

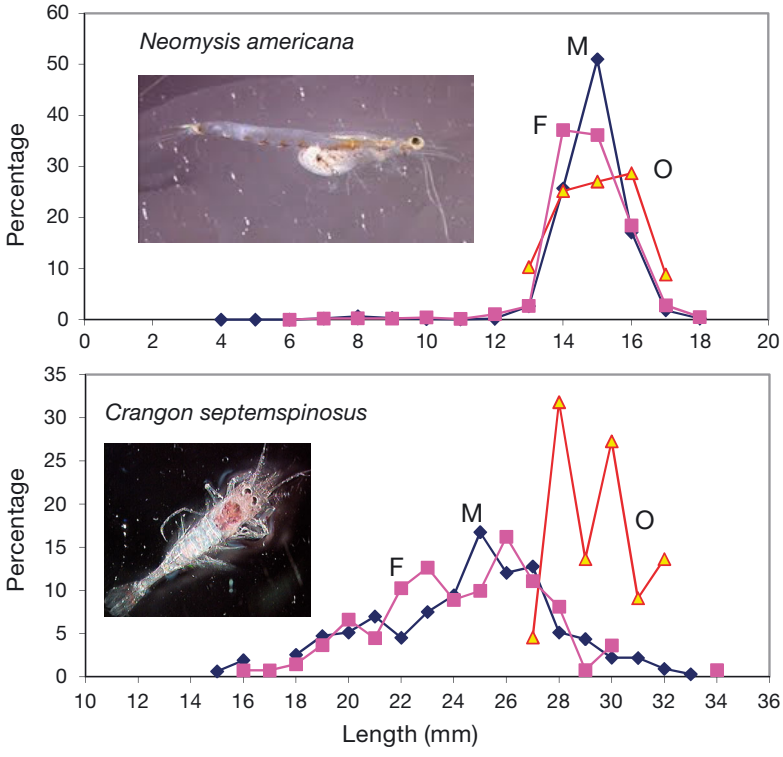

Fig. 5. Percentage length frequencies of *Neomysis americana* (upper panel) and *Crangon septemspinosus* (lower panel) from five 10 m MOCNESS tows on the southeastern Georges Bank from 17 to 19 June 1985. Males (M), females (F) and ovigerous females (O) are shown

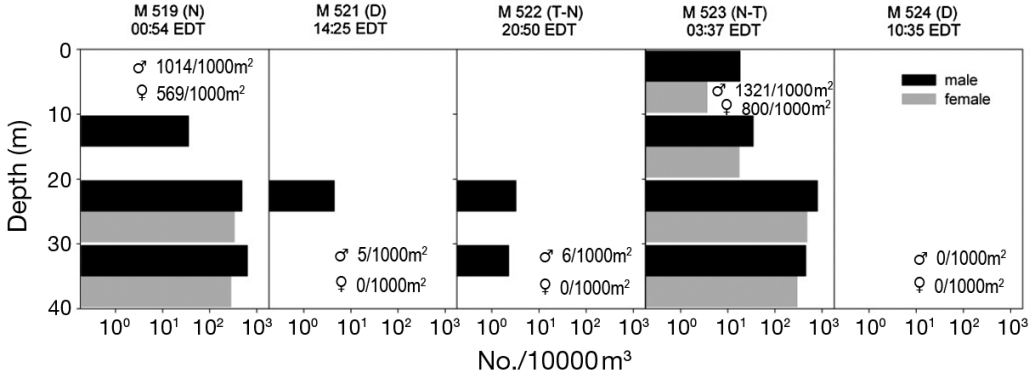

Fig. 6. Vertical distribution of *Crangon septemspinosus* from five 10 m MOCNESS tows at a location on the southeastern Georges Bank from 17 to 19 June 1985. Water depths ranged from 43 to 49 m. The MOCNESS tow number and time mid-point are located above each column and designated as night (N), day (D), or twilight (T) in parentheses. EDT: Eastern Daylight Time. Male (black) and female (gray) densities are shown as separate bars within a 10 m stratum. Note the $\log_{10}$ density scale. Water column abundances (no./1000 m^2) of males and females are included below each tow panel

long-term mean, while the velocity in the north–south direction (V) was 25 to 40% larger than the climatology value over Georges Bank. Velocity shear in the vertical was expected to have minimal interannual variability, as tidal flows control the circulation over Georges Bank.

The flow on the southern flank is affected by the presence of the tidal front, which modifies both vertical and horizontal patterns of circulation. Recirculation cells associated with the front have been described previously (Garrett & Loder 1981, Lynch et al. 1992, Aretxabaleta et al. 2005) and were evident in the average circulation during June 1985 (Fig. 7). The main features of the secondary flow are: upwelling in the mixed region (on-bank of the front), downwelling in the stratified region (off-bank of the front), convergence near the surface and divergence near the bottom. The strong tidal front jet flow exhibited along-bank velocities in excess of 15 cm s^{-1} flowing southwest on the southern flank, with peak speeds in 60 and 80 m water depths (Fig. 7).

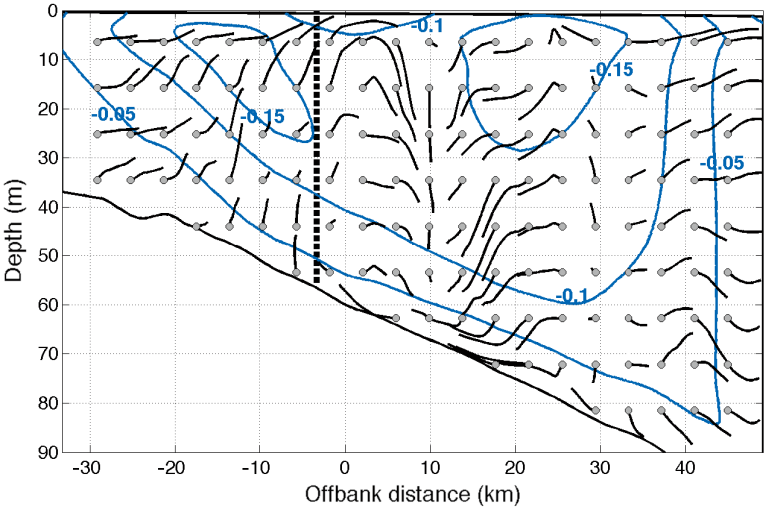

Fig. 7. Trajectories of passive drifters in a vertical transect across the southern flank using averaged flow fields over 16 d. The particle trajectories were integrated for 3 d. Gray circles represent the original release positions of the model drifters. Blue lines are contours of normal velocity, with negative values representing southwestward flow. Vertical dashed black line represents an estimate of the mean tidal front position over the 16 d average period given by the Simpson-Hunter tidal mixing parameter (Simpson & Hunter 1974). The (dimensionless) value of $h/\rho \cdot C_D \cdot u^3$ used is $10^{1.9}$ (Garrett et al. 1978, Lynch & Naimie 1993), where h is the water column depth, ρ is the density of seawater, C_D is a drag coefficient taken as 0.0027 and u is the RMS (root-mean-square) size of the velocity over the simulated period. The x-axis corresponds to the distance off-bank from the 60 m isobath

Particle-tracking simulations

To assess the quality of particle-tracking simulations, observed vertical distributions were interpolated in time to cover the entire daily cycle. We assumed that the near disappearance of migrating shrimp from the field time-series was caused by individuals being on or near the bottom, below the maximum sampling depth of the MOCNESS. It is possible that the shrimp population was displaced from the sampling site during the day tows; however, their diel vertical pattern conforms to the expected behavior noted in other studies. It is unknown whether individuals remain at depth or whether a continuous exchange of individuals takes place throughout the water column. Since the MOCNESS time-series were made at a well-mixed site, we are unsure of the vertical distribution of shrimp at a stratified location on the southern flank. Is their migratory behavior modified by the near-surface thermocline or the declining strength of the bottom tidal current with depth? In these simulations we assumed the inferred migratory behavior would be the same in mixed and stratified water columns. The average (male and female) hourly density distributions as a function of time of day are shown in Fig. 8. As the total observed population inventory varies considerably during the day, instead of using density for comparison with the simulated particles, a percentage of the total number of particles observed at any time (Fig. 8B,D) was used as a metric of the vertical distribution for comparisons with the particle-tracking results. The percentage

Table 3. Comparison between climatological and 1985 RMS (root-mean-squared) wind speeds (m s^{-1}) at NDBC Buoy 44011. Comparison between the FVCOM (finite volume coastal ocean model) and climatology depth-averaged RMS speeds (m s^{-1}) at the MOCNESS sampling location. U: velocity in the east–west direction; V: velocity in the north–south direction

	Wind		Total depth averaged		Sub-tidal depth averaged	
	U	V	U	V	U	V
Climatology						
Jun	3.68	4.08	0.40	0.52	0.03	0.08
Jul	3.19	3.86	0.41	0.55	0.04	0.06
1985						
Jun	3.58	4.04	0.43	0.54	0.04	0.10
Jul	2.83	4.08	0.42	0.54	0.05	0.11

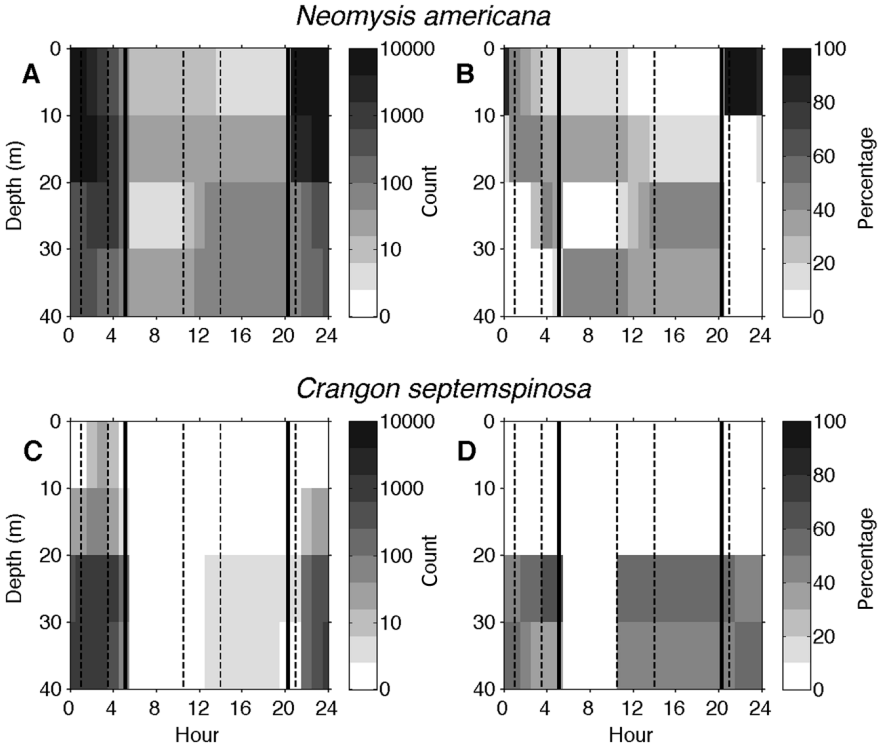

Fig. 8. Vertical distributions of the density of (A,B) *Neomysis americana* and (C,D) *Crangon septemspinosus* as an average of both males and females as a function of time of day. The left panels represent total counts, and the right panels show the percentage of the total density present for each bin depth at each time (i.e. the sum of the percentage in the vertical is 100% for each time). The times of sunrise and sunset are indicated by vertical solid lines, and the sampling times, by thin dashed lines

distribution clearly showed the presence of *C. septemspinosus* in the deeper part of the water column, with most of the total population concentrated below 20 m, even at night. Meanwhile, the rapid upward migration and concentration of *N. americana* at 0 to 10 m at dusk was even more evident, while, during the day, a large fraction (between 20 and 40%) of the population in the water column was observed above the deepest bin, even though the abundance was small during that time.

The horizontal distribution of particles in the basic simulation varied slightly from that in simulations taking behavior into consideration (Fig. 9). The integrated pathway over 30 d of tracking showed that particles released without behavior (basic simulation) completed a full loop around the Bank, with particles found predominantly between the 40 and 80 m isobaths on the southern flank and with some travelling to depths deeper than 150 m on the northern flank. The highest percentage of total particles was found in the area associated with the tidal front.

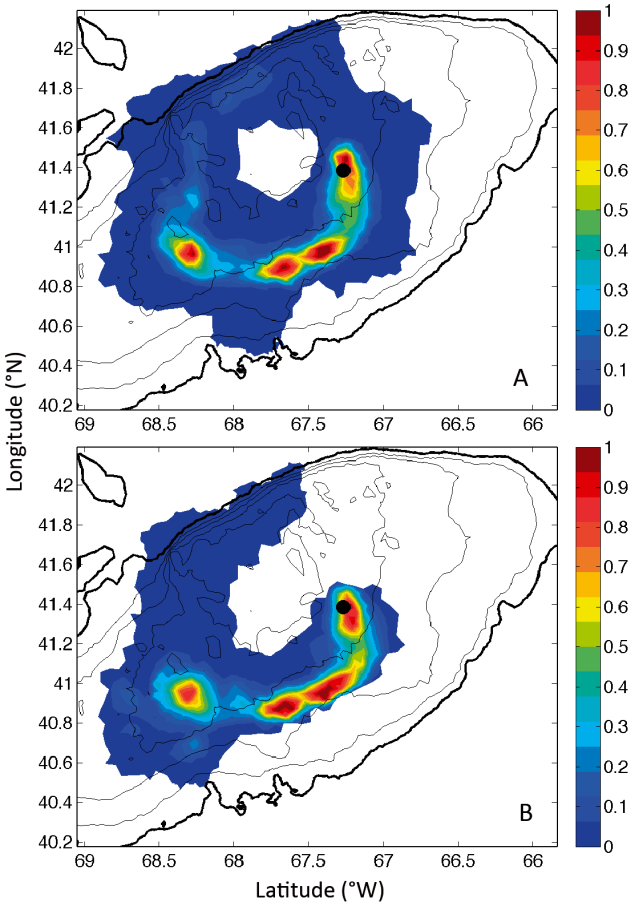

Fig. 9. Spatial distribution of the percentage of total particles in each model grid element after 30 d of tracking: (A) simulation without behavior and (B) simulation with 5 mm s^{-1} vertical swim speed. The black circle indicates the initial location of release. The black contours mark the 40, 60, 80, 100 and 150 m isobaths. The color bar indicates percentage

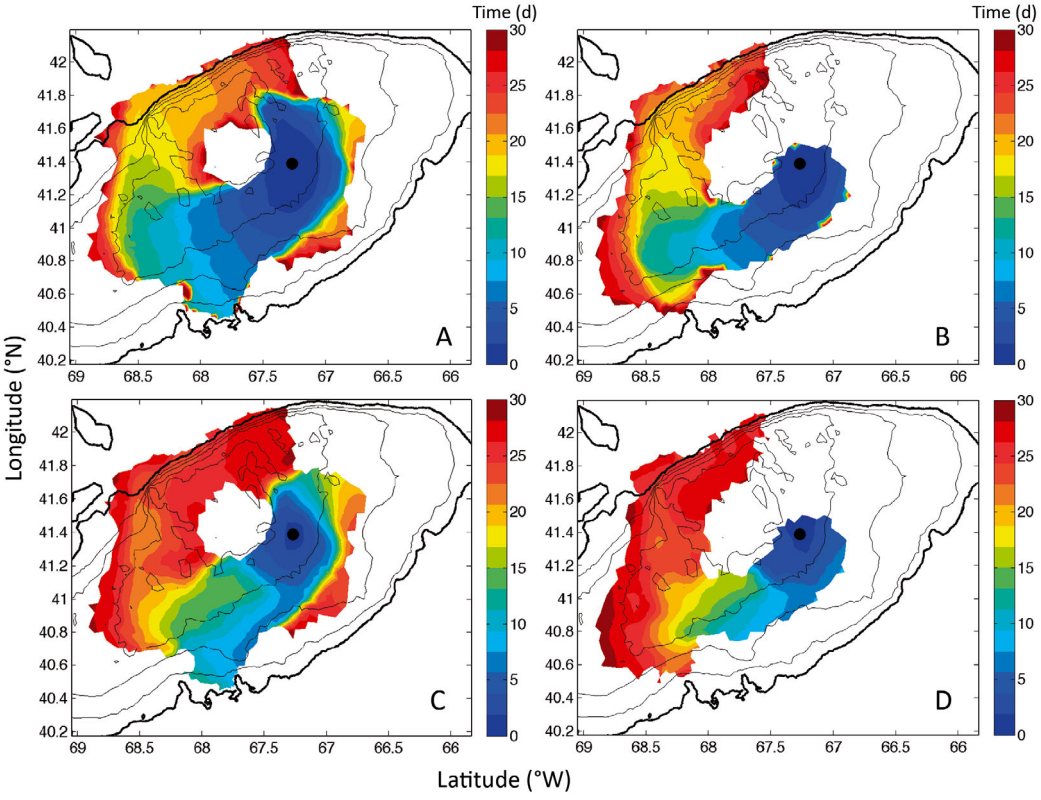

Fig. 10. Upper panels: time of 1st arrival (days) to each location for particles: (A) without behavior and (B) with 5 mm s^{-1} swim speed. Lower panels: average time of arrival to each location for particles: (C) without behavior and (D) with 5 mm s^{-1} swim speed. The black contours mark the 40, 60, 80, 100 and 150 m isobaths. The color bar indicates days from release

When behavior was added (5 mm s^{-1} swim speed) to the simulations, the area covered by the particles was reduced and the particles did not complete the loop around the Bank in 30 d. The cross-bank extent was also slightly limited, with higher percentages found associated with the tidal front.

To estimate how the different areas of Georges Bank were connected, 2 estimates of travel time were considered. The first estimate was the shortest time that it took any particle to reach a specific location (Fig. 10A,B), while the second estimate considered the average time for all particles to reach a location (Fig. 10C,D). The time of first arrival for the simulation with no behavior showed an almost isotropic distribution within the first 2 d, a broadening tail that reached the southern edge of the Bank in 7 d and predominantly turned north around Day 10, with the first particles completing the full loop in around 25 d. The time of first arrival in the simulation with 5 mm s^{-1} swim speed showed particles moving predominantly south during the first 2 d, with a narrower tail confined to areas shallower than 80 m in the first 10 d. When the particles reached the Great South Channel area, they started either crossing to deeper isobaths across the Channel or being incorporated into the northern flank, where the steeper topography contributed to the cross-isobath exchange.

When average time was considered, the particles that reached the southern edge (crossing the 80 m isobath) in the basic simulation presented short (6 to 10 d) averaged times, suggesting that an initial particle loss had occurred (associated with initial cross-frontal export) but that most particles tended to remain in the domain. The average time to complete the loop around the Bank was around 27 to 30 d. In the simulation with 5 mm s^{-1} swim speed, the average time to reach any location was almost always slightly longer than in the basic case.

As some particles in the basic run completed the loop, the average time metric for the long 30 d simulation was not optimal, since some areas were averaging particles near the initial location with particles that had travelled around the Bank. To alleviate this problem, shorter simulations lasting for 16 d were considered (Fig. 11). The simulation with no behavior (Fig. 11A) exhibited particles reaching their westernmost extent after 16 d, just before starting to move northward. A branch of particles also existed that

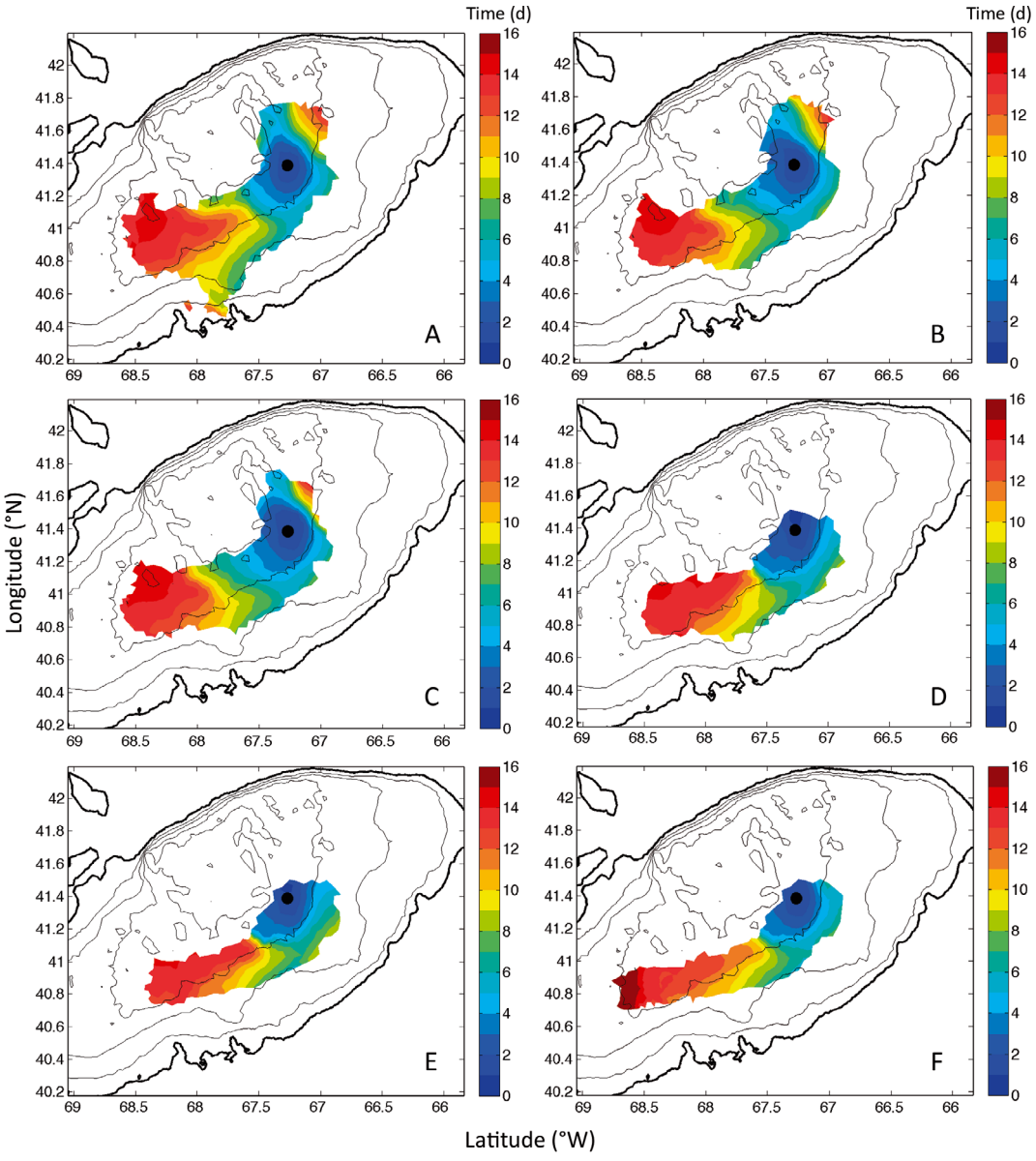

Fig. 11. Average time (days) of arrival for particles tracked over 16 d: (A) without behavior and diel migration with swim speeds of (B) 1 mm s^{-1}, (C) 2 mm s^{-1}, (D) 5 mm s^{-1}, (E) 10 mm s^{-1} and (F) 20 mm s^{-1}. The black contours mark the 40, 60, 80, 100 and 150 m isobaths. The color bar indicates days from release

was initially transported toward shallower Bank areas. The distribution of particles at 0.5 mm s^{-1} swim speed was similar to the distribution with no behavior (not shown). The simulation with 1 mm s^{-1} swim speed restricted the southward motion of the branch that reached the southern edge of the Bank in the basic simulation, resulting in almost no particles travelling across the 80 m isobath (Fig. 11B). The horizontal spread of particles from the simulation with 2 mm s^{-1} swim speed (Fig. 11C) was slightly smaller in size than that of the 1 mm s^{-1} simulation, but the time distribution was similar. The 5 mm s^{-1} simulation (Fig. 11D) exhibited a narrower path, with particles being less likely to be near the 40 m isobath and little transport of particles toward shallower areas. The simulation with 10 mm s^{-1} vertical speed (Fig. 11E) showed the narrowest spatial distribution, but there were a limited number of particles near the 40 m isobath outside the initial release location. Most particles were concentrated in an area centered around the 60 m isobath, where the tidal front was located. The simulation with 20 mm s^{-1} swim speed (Fig. 11F) exhibited a similar concentration near the 60 m isobath, but with some particles tending to be trans-

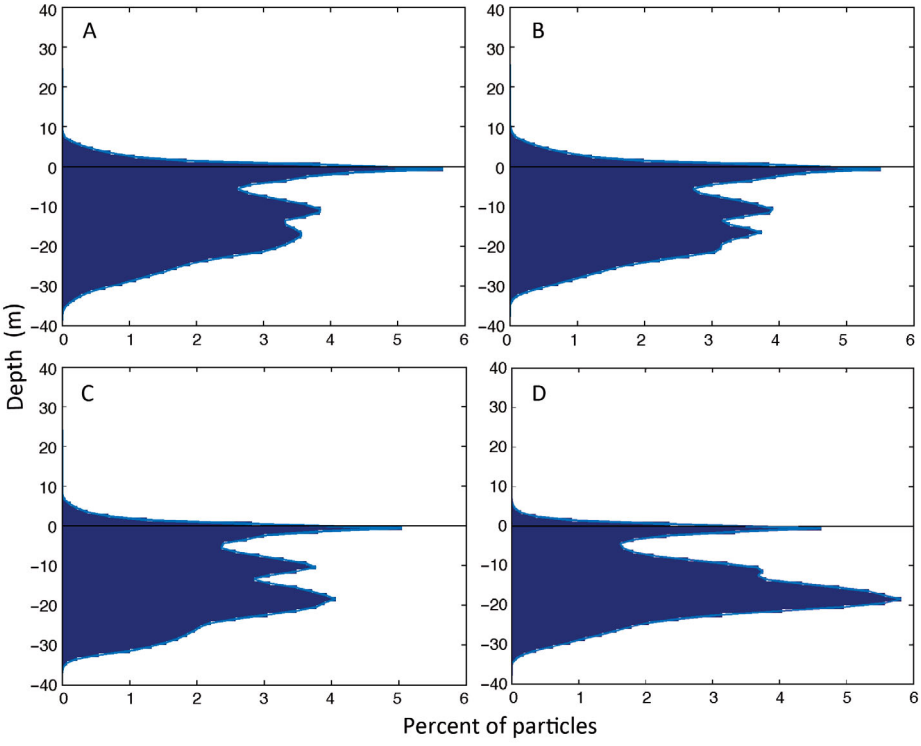

Fig. 12. Cross-bank depth change as histograms of the percentage of total number of particles for the 16 d simulations with: (A) no behavior, (B) 1 mm s^{-1}, (C) 5 mm s^{-1} and (D) 10 mm s^{-1} swim speeds. The histogram bins are 1 m thick. Positive (negative) values indicate on-bank (off-bank) displacement

ported west toward the Great South Channel in periods of around 15 d.

Cross-bank particle displacement (Fig. 12) was estimated as the change in bottom depth from the original release isobath (between 43 and 46 m). In general, in the 16 d simulations, particles remained 10 m shallower to 40 m deeper than the depth of their release location. The largest peaks were for no cross-bank displacement (zero isobath change) in all 16 d simulations, except in the cases of 10 mm s^{-1} (Fig. 12D) and 20 mm s^{-1} swim speeds (not shown). The basic simulation showed off-bank dis-

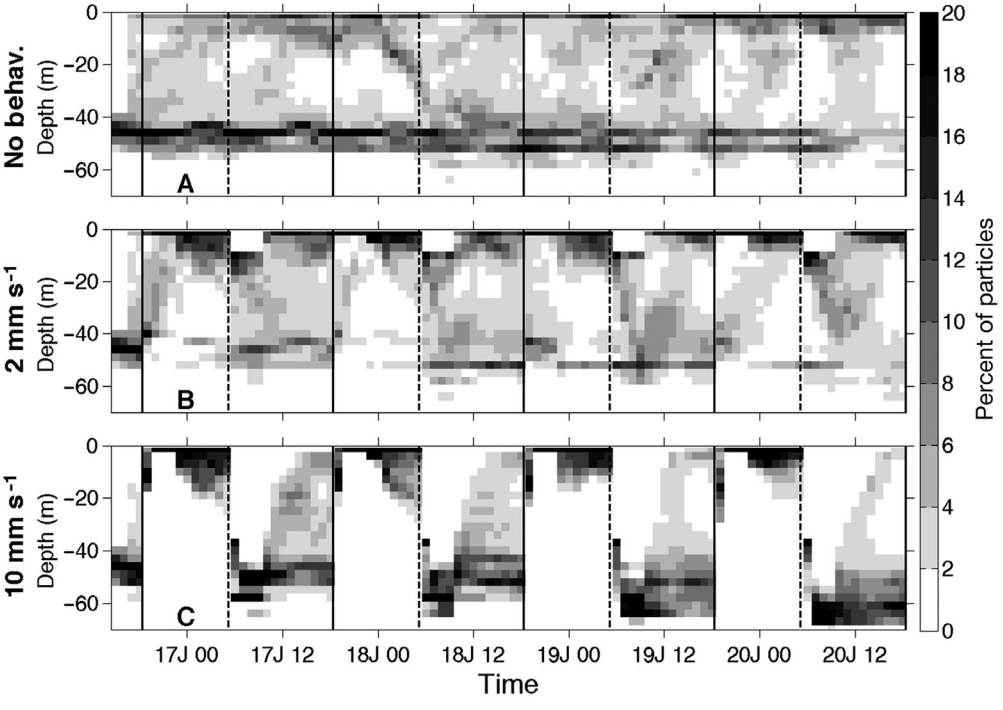

Fig. 13. Vertical distributions of model particles (percentage of total at any time) during 4 d (16 June, 18:00 to 20 June, 18:00) integrated over the entire horizontal domain: (A) no behavior, (B) 2 mm s^{-1} and (C) 10 mm s^{-1} swim speeds. The format of the *x*-axis is day-June (J)-midnight (00) or noon (12)

Table 4. Percentage of particles found at water depths shallower than 60, 70 and 80 m. The 3 chosen depths represent locations 15, 25 and 35 m deeper than the original release depth (43 to 46 m) in simulations lasting 16 d

	No vert. migration	Vertical swim speed (mm s^{-1})					
		0.5	1	2	5	10	20
<60 m	65.0	65.9	66.7	68.4	57.0	53.1	45.3
<70 m	93.5	94.4	94.9	95.7	93.6	93.8	89.3
<80 m	97.9	98.9	99.3	99.9	99.5	99.1	95.3

Table 5. Percentage difference (RMS) between the simulated particle vertical distribution in time and the vertical distribution of *Neomysis americana* and *Crangon septemspinosus* presented in Fig. 8

	No vert. migration	Vertical swim speed (mm s^{-1})					
		0.5	1	2	5	10	20
N. americana	27.8	26.1	24.1	23.5	22.5	19.8	23.3
C. septemspinosus	41.5	40.4	39.2	36.0	39.7	41.4	45.1

placement peaks at 10 and 18 m. While the simulation with a 1 mm s^{-1} swim speed exhibited a similar peak distribution to that of the basic simulation, its total offshore displacement was smaller. The simulation with 5 mm s^{-1} swim speed showed an increase of off-bank movement which increased in the 10 mm s^{-1} simulation, where the largest percentage of particles resided 18 m off-bank of the release location.

The relative distribution of model particles in the vertical (Fig. 13) exhibited marked differences depending on the presence or absence and magnitude of swimming behavior. While the particles with no behavior tended to remain confined to the near-surface and, especially, near-bottom areas due to vertical velocities caused by tidal fluctuations, the particles with 10 mm s^{-1} swim speed experienced a rapid transition from the surface to the bottom in narrow vertical layers. The particles with 2 mm s^{-1} swim speed spent considerably more time in the central part of the water column. There was a tendency to find particles in deeper areas (they were released around the 45 m isobath) as time passed, especially in the particles with fast swim speeds; these results were consistent with cross-bank particle displacements (Fig. 12).

Retention was estimated as a percentage of total particles found in areas shallower than the 60, 70 and 80 m isobaths (15, 25 and 35 m deeper than the release depth of about 45 m; Table 4). The highest retention in areas as far as 15 m below the original release depth was for the simulation with 2 mm s^{-1} swim speed, while minimum retention occurred in the simulation with 20 mm s^{-1} swim speed. The same response was also observed when retention was estimated based on particles found in areas no deeper than 25 or 35 m below the original release location. In 16 d <5% particle loss was estimated for areas shallower than 35 m from the release depth for the worst-case scenario (20 mm s^{-1}), while the rest of the simulation lost between 0.1 and 2%.

The modeled vertical distribution was calculated by dividing the water column into 4 bins that spanned the entire water column at each horizontal location and then averaging overall areas where particles were found. The skill of the modeled particle distribution was examined by comparing the modeled vertical structure and the interpolated observed structure of *N. americana* and *C. septemspinosus* (Fig. 8). Precision was estimated as the total RMS difference between the percentages obtained from the model and observations of the 4 separate bins.

The vertical swimming speed for *N. americana* in the numerical simulations that best matched (smaller global RMS difference) the interpolated observed vertical distribution (Fig. 8) after the 16 d simulation was 10 mm s^{-1}, whereby the numerical particles reproduced >80% of the observed variability (Table 5). For *C. septemspinosus*, the differences between numerical and observed distributions were much larger and the greatest precision (smaller RMS) was achieved in the simulation with 2 mm s^{-1} swim speed (similar precision was obtained with 1 mm s^{-1}). The percentage variability reproduced was around 57%. The reduced precision was associated with the fact that the vertical distribution of observed *C. septemspinosus* was restricted to the lower part of the water column, while that limitation was not imposed on the simulated particles.

For the 20 mm s^{-1} simulation, particles were moving too rapidly from the bottom to the surface for our purposes, and the fast vertical velocity (equivalent to 72 m h^{-1}) overshadowed any vertical turbulent displacement. In the resulting profile, particles were either near the surface or near the bottom and we were not able to properly reproduce the observed profile.

DISCUSSION

Georges Bank shrimp appear to respond primarily to light, as tidal currents are a relatively constant semi-diurnal rotary. The 5 vertical profiles of the *Neomysis americana* and *Crangon septemspinosus* adults located at the tidal front on Georges Bank during June 1985 presented a diel pattern of vertical migration, the rates and dispersal of which were explored here though particle releases in a modeled flow field. Basic runs of FVCOM included simulated temperature, salinity, tidal and wind information for June 1985, and the circulation profile we obtained was close to the previously reported average conditions during that month. The vertical profiles at the end of the simulations were compared to the observed vertical day–night MOCNESS profiles to determine the closest vertical migration rate. The consequences of different vertical ascent and decent swim speeds were determined by the horizontal dispersion of particles over 30 d. Unfortunately, there was no sufficiently dense grid of observational survey station data against which to compare the horizontal model simulation results.

The model simulations indicated that some vertical behavior was required to match the observed vertical profiles. The best match (smaller RMS difference; Table 5) for *N. americana* was with a swimming speed of 10 mm s^{-1}; however, the best match for *C. septemspinosus* was with 2 mm s^{-1}. *N. americana* rapidly moved up to the surface at twilight (10 mm s^{-1}), where they appeared to redistribute in the water column by night and then quickly retreat to the bottom by first light. *C. septemspinosus* also appeared to migrate at twilight, but at a slower speed (2 mm s^{-1}), and they stayed in the lower part of the water column at night. These migration rates were within the range estimated from the 17 to 19 June 1985 Chromscope scattering observations, 8.2 to 9.4 mm s^{-1}, for *N. americana*. Since *C. septemspinosa* only migrates from the bottom to mid-depth and back, its rate may be about half that of *N. americana*, or about 4 to 5 mm s^{-1}. *C. septemspinosus* is larger and heavier than *N. americana*, which may be a factor in their slower migration, or they may exhibit a different behavior, such as reacting more slowly to a given light level or change. Their emergence also may also follow the migration of *N. americana*, since *Crangon* spp. are known to be prominent predators of mysids when they are abundant (Siegfried 1982, Taylor et al. 2005).

The highest retention of particles on the Bank (Table 4) was achieved using the 2 mm s^{-1} swim speed, but more particles were still located in the immediate vicinity of the tidal front using swimming speeds of 10 to 20 mm s^{-1} (Fig. 11). Particles that spent more time near the surface were more likely to be closely associated with the tidal front because of near-surface convergence, but were also transported further inside the tidal jet and were more likely to ultimately escape the Bank. Therefore, adult *N. americana* are expected to be more associated with the tidal front, while *C. septemspinosus* adults are more likely to be retained on the Bank (areas shallower than 80 m), since they are found deeper in the water column both day and night. The spring–neap tidal fluctuations (not shown) introduced more retention variability in a typical June than the interannual fluctuations, as tides remained the main driving force of the flow over Georges Bank. The conditions during June 1985 were typical for the stratified season on the Bank (Table 3), but seasonal and interannual fluctuations alter the position and strength of the tidal front, changing the potential for retention (Naimie et al. 1994, Naimie 1996, Lough et al. 2006b). Individuals transported farther west to the Nantucket shoals and Mid-Atlantic Bight can still find other suitable habitats on the shelf for their survival (Theroux & Wigley 1998). Different behaviors by the 2 species confer different advantages in relation to the tidal front. Aggregation in the area of the front presumably enhances mating and feeding, but being in the surface jet or closer to the bottom results in different patterns of retention or transport from the bank, or from suitable habitat. The contribution of random displacements to the final position is minimized, as the vertical and horizontal diffusivities are reduced in the proximity of the tidal front, where advective dynamics dominate. Spreading the risk by spawning over a wider area and longer period is a reproductive strategy to counter loss in a variable environment that both species use. Another adaptation would be to have a shorter larval period until juvenile settlement. *N. americana* females carry eggs and larvae in brood pouches until they are released as juveniles, which may compensate for their greater potential surface transport and loss from the Bank.

Several previous studies have analyzed the retention of passive particles on Georges Bank under different conditions. Werner et al. (1993) identified the region of highest retention on the Bank using model simulations, which coincided with the region of highest growth rate and highest survival for larval cod and haddock (Werner et al. 1996). Lough & Manning (2001) provided a general description of the tidal front jet and the cross-bank exchanges on the southern flank. Aretxabaleta et al. (2005) examined the

cell-like circulation in the frontal region during May 1999 that enhanced passive particle retention in the proximity of the tidal front on the southern flank. Lough et al. (2006a) modeled growth of Atlantic cod larvae under the circulation associated with the tidal front and found marked growth differences between the stratified and mixed sides of the front. Lough et al. (2006b) used an 11 yr time-series (1977 to 1987) of cod and haddock egg/larval distributions to describe the differences between the eastern and western areas of Georges Bank and the interannual variability in retention.

Environmental cues that may initiate, control, and/or modify vertical swimming behavior may change with developmental stage and the depth of the water column, as reported in studies on related species. A review of the literature on the behavior of penaeid prawns found that most burrow into the substratum during the day and emerge at night, responding to environmental factors such as light, tide and temperature (Dall et al. 1990). Their larvae have an endogenous diel migratory behavior, rising in the water column at night and descending during the day. Emigration into estuaries by epi-benthic post-larvae has been related to the day/night cycle for some species, whereby a portion of the population emerges into the water column at night, coinciding with the flood tide. Other species may use selective tidal stream emigration, which depends on post-larvae sensing environmental cues in estuarine gradients such as salinity, turbidity and organic matter. Rothlisberg et al. (1995) monitored the vertical migratory behavior of post-larval *Penaeus plebejus* in southeast Queensland, Australia, and provided evidence for a conservative mechanism that allows post-larvae to enter a nursery area without sensing estuarine gradients. They proposed that post-larvae in the nearshore region change from a diurnal vertical migration pattern to a tidal vertical migration pattern by being able to sense the relative difference in tidal pressure. Post-larvae buried in the sediment would ascend into the water column during the flood current pressure cue and then settle out after a short period determined by an endogenous clock, also initiated by the tidal pressure cue. Similarly, pink shrimp (*Farfantepenaeus duorarum*) post-larvae were predominantly caught during the dark flood period leading into the western Florida Bay nursery area, indicating their vertical movement had changed in response to the stage of tidal flow (Criales et al. 2006). Laboratory experiments have shown post-larvae to change behavior in relation to pressure and salinity changes.

The blue crab *Callinectes sapidus* also has a complex life cycle, whereby larvae are transported from offshore on the Atlantic shelf to nearshore by wind-driven circulation and then into estuaries as post-larvae (megalopae) by flood tide transport, where they settle and metamorphose to early juvenile stages (Forward et al. 2007). Megalopae and juveniles exhibit endogenous vertical swimming activity, ascending up the water column at night and descending during the day; however, their response to environmental factors controls the onset and duration of vertical migration during flood tides.

N. interger is found most abundantly in low-flow areas in the field (Ythan estuary, northeast Scotland) and avoids areas of high flow based on laboratory experiments (Lawrie et al. 1999). Speirs et al. (2002) attempted to predict the migratory behavior of *N. interger* through strategic modeling designed to examine the random movement hypothesis, foraging hypothesis, and depth-seeking/predation hypothesis, and to compare model results with field and laboratory studies. These hypotheses were rejected or weakly supported by the evidence, so they hypothesized that the behavioral response to flow was most likely the proximate cause determining the distribution of this species over the intertidal zone.

On the other hand, no evidence was found by Kringel et al. (2003) for a strong tidal modulation of light on emergence or reentry of *N. kadiakensis* in the 20 to 25 m deep Puget Sound, Washington. Mean swimming speeds of accent and decent ranged from 0.59 to 0.96 cm s^{-1}. Group migration speed was estimated at 0.34 to 1.37 cm s^{-1}, which is much slower than maximum swimming or cruising speeds, suggesting that ascent and descent were regulated by ambient light intensities. Ascent and decent were symmetrical in space and time, with similar rates of vertical movement. Mysids (2 to 21 mm in length) ascended to the upper water column but were still spread throughout the water column during night.

Daewel et al. (2011) modeled the transport of brown shrimp (*Crangon crangon*) post-larvae and juveniles, spawned at depths between 10 and 30 m in the German Bight, according to various tidal cues to determine the selective tidal-stream transport necessary for juvenile settlement. They showed that hydrodynamic forces exerted by strong tidal currents on the flat-bodied shrimp could be sufficient to provide vertical lift in the water column for selective tidal stream transport. In this case, the shrimp did not have to swim to the surface, since tidal-current shear is at a minimum in the central part of the water column. Their hypothesis of tidally induced vertical lift

without swimming might also partially explain why *C. septemspinosus* only ascended to mid-depth in the Georges Bank samples in contrast to *N. americana*. However, the vertical lift effect is not considered the proximate control of vertical migration, since there are strong rotary tidal currents on Georges Bank and observations indicated that the migration activity of both species was associated with the day–night cycle. The Daewel et al. (2011) simulations did not include diel migratory behavior as a function of light. Other studies cited in the 'Introduction' document that diel behavior is related to the light cycle, supporting the MOCNESS vertical profile observations in June 1985, which showed that the adults of both species are found throughout the water column at night and absent during the day on Georges Bank at 43 at 49 m bottom depth. In various previous studies cited in this paper, the environmental factors that act as initiating, controlling, or modifying variables appear to depend on the species' stage and on adaptation to their local habitat.

SUMMARY

The Georges Bank simulations conducted in this study provided reasonable vertical migration rates that matched the observed vertical profiles over a day–night cycle for the 2 shrimp species *Crangon septemspinosus* and *Neomysis americana*. They provided support for *N. americana* being more closely associated with the tidal front, since that species is found more abundant near the surface during the night and, thus, is subjected to near-surface, tidal-front convergence. In contrast, *C. septemspinosus* resides primarily in the lower part of the water column, below the near-surface, southwestward-flowing tidal jet. However, the consequences of their different vertical behaviors in the June 1985 flow field show *N. americana* to have less retention on Georges Bank than does *C. septemspinosus*, which resides closer to the bottom. Further simulations require more information on the life history of the 2 species.

Acknowledgements. We thank E. Broughton for making MOCNESS vertical distribution figures. Changsheng Chen (UMASS Dartmouth) provided the FVCOM hindcast online at the archive www.smast.umassd.edu:8080/thredds/dodsC/fvcom/hindcasts/30yr_gom3.html. We appreciate the helpful comments provided by John Hare (NOAA) and Brad Butman (USGS). Any use of trade, firm, or product names is for descriptive purposes only and does not imply endorsement by the US Government.

LITERATURE CITED

Abello HU, Shellito SM, Taylor LH, Jumars PA (2005) Light-cued emergence and re-entry events in a strongly tidal estuary. Estuaries 28:487–499

Al-Adhub AHY, Naylor E (1975) Emergence rhythms and tidal migrations in the brown shrimp *Crangon crangon* (L.). J Mar Biol Assoc UK 55:801–810

Aretxabaleta A, Manning J, Werner FE, Smith K, Blanton BO, Lynch DR (2005) Data assimilative hindcast on the southern flank of Georges Bank during May 1999: frontal circulation and implications. Cont Shelf Res 25:849–874

Aretxabaleta AL, Butman B, Signell RP, Dalyander PS, Sherwood CR, Sheremet VA, McGillicuddy DJ Jr (2014) Near-bottom circulation and dispersion of sediment containing *Alexandrium fundyense* cysts in the Gulf of Maine during 2010–2011. Deep-Sea Res II 103:96–111

Blanton BO (1993) User's manual for 3-dimensional drogue tracking on a finite element grid with linear finite elements. Technical Report, UNC Marine Sciences, Chapel Hill, NC

Brown H, Bollens SM, Madin LP, Horgan EF (2005) Effects of warm water intrusions on populations of macrozooplankton on Georges Bank, Northwest Atlantic. Cont Shelf Res 25:143–156

Chen C, Lui H, Beardsley RC (2003) An unstructured, finite-volume, three-dimensional, primitive equation ocean model: application to coastal ocean and estuaries. J Atmos Ocean Technol 20:159–186

Criales MM, Wang JD, Browder JA, Robblee MB, Jackson TL, Hittle C (2006) Variability in supply and cross-shelf transport of pink shrimp (*Farfantepenaeus duorarum*) postlarvae into western Florida Bay. Fish Bull 104:60–74

Daewel U, Schrum C, Temming A (2011) Towards a more complete understanding of the life cycle of brown shrimp (*Crangon crangon*): modeling passive larvae and juvenile transport in combination with physically forced vertical juvenile migration. Fish Oceanogr 20:479–496

Dall W, Hill BJ, Rothlisberg PC, Staples DJ (1990) The biology of Penaeidae. Adv Mar Biol 27:1–489

Forward RB Jr, Diaz H, Ogburn MB (2007) The ontogeny of the endogenous rhythm in vertical migration of the blue crab *Callinectes sapidus* at metamorphosis. J Exp Mar Biol Ecol 348:154–161

Fulton RS III (1982) Preliminary results if an experimental study of the effects of mysid predation on estuarine zooplankton community structure. Hydrobiologia 93:79–84

Garrett CJR, Keely JR, Greenberg DA (1978) Tidal mixing versus thermal stratification in the Bay of Fundy and Gulf of Maine. Atmosphere-Ocean 16:403–423

Hartsuyker L (1966) Daily tidal migrations of the shrimp, *Crangon crangon.* Neth J Sea Res 3:52–67

Herman SS (1963) Vertical migration of the opossum shrimp, *Neomysis americana* Smith. Limnol Oceanogr 8:228–238

Jumars PA (2007) Habitat coupling by mid-latitude, subtidal, marine mysids: import-subsidised omnivores. Oceanogr Mar Biol Annu Rev 45:89–138

Kringel K, Jumars PA, Holliday DV (2003) A shallow scattering layer: high resolution acoustic analysis of nocturnal vertical migration from the seasbed. Limnol Oceanogr 48:1223–1234

Lawrie SM, Speirs DC, Raffaelli DG, Gurney WSC, Paterson DM, Ford R (1999) The swimming behaviour and distribution of *Neomysis interger* in relation to tidal flow. J Exp Mar Biol Ecol 242:95–106

Li Y, He R, Manning JP (2014) Coastal connectivity in the Gulf of Maine in spring and summer of 2004–2009. Deep-Sea Res II 103:199–209

Link JS, Garrison LP (2002) Trophic ecology of Atlantic cod *Gadus morhua* on the northeast US continental shelf. Mar Ecol Prog Ser 227:109–123

Loder JW, Wright DG (1985) Tidal rectification and frontal circulation on the sides of Georges Bank. J Mar Res 43: 581–604

Lough RG, Manning JP (2001) Tidal-front entrainment and retention of fish larvae on the southern flank of Georges Bank. Deep-Sea Res II 48:631–644

Lough RG, Broughton EA, Buckley LJ, Incze LS and others (2006a) Modeling growth of Atlantic cod larvae on the southern flank of Georges Bank in the tidal-front circulation during May 1999. Deep-Sea Res II 53:2771–2788

Lough RG, Hannah CG, Berrien PL, Brickman D, Loder JD, Quinlan JA (2006b) Spawning pattern variability and its effect on retention, larval growth and recruitment in Georges Bank cod and haddock. Mar Ecol Prog Ser 310: 193–212

Lynch D, Naimie C (1993) The M_2 tide and its residual on the outer banks of the Gulf of Maine. J Phys Oceanogr 23: 2222–2253

Lynch DR, Werner FE, Greenberg DA, Loder JW (1992) Diagnostic model for baroclinic, wind-driven and tidal circulation in shallow seas. Cont Shelf Res 12:37–64

Mauchline J (1980) The biology of mysids and euphausiids. Adv Mar Biol 18:1–681

Mellor GL, Yamada T (1982) Development of a turbulence closure model for geophysical fluid problems. Rev Geophys Space Phys 20:851–875

Mitarai S, Siegel DA, Watson JR, Dong C, McWilliams JC (2009) Quantifying connectivity in the coastal ocean with application to the Southern California Bight. J Geophys Res 114:C10026, doi:10.1029/2008JC005166

Naimie CE (1996) Georges Bank residual circulation during weak and strong stratification periods: prognostic numerical model results. J Geophys Res 101(C3): 6469–6486

Naimie CE, Loder JW, Lynch DR (1994) Seasonal variation of the three-dimensional residual circulation on Georges Bank. J Geophys Res 99(C8):15967–15989

Price KS (1962) Biology of the sand shrimp, *Crangon septemspinosa*, in the shore zone of the Delaware Bay region. Chesap Sci 3:244–255

Richards SW, Riley GA (1967) The benthic fauna of Long Island Sound. Bull Bingham Oceanogr Collect 19:89–129

Rothlisberg PC, Church JA, Fandry CB (1995) A mechanism for near-shore concentration and estuarine recruitment of post-larval *Penaeus plebejus* Hess (Decapoda, Penaeidae). Estuar Coast Shelf Sci 40:115–138

Sato M, Jumars PA (2008) Seasonal and vertical variations in emergence behaviors of *Neomysis americana.* Limnol Oceanogr 53:1665–1677

Siegfried CA (1982) Trophic relations of *Crangon franciscorum* Stimpson and *Palaemon macrodactylus* Rathbun: predation on the opossum shrimp, *Neomysis mercedis* Holmes. Hydrobiologia 89:129–139

Simpson JH, Hunter JR (1974) Fronts in the Irish Sea. Nature 250:404–406

Smagorinsky J (1963) General circulation experiments with the primitive equations. I. The basic experiment. Mon Weather Rev 91:99–164

Speirs D, Lawrie S, Raffaelli D, Gurney W, Emes C (2002) Why do shallow-water predators migrate? Strategic models and empirical evidence from an estuarine mysid. J Exp Mar Biol Ecol 280:13–31

Taylor LH, Shellito SM, Abello HU, Jumars PA (2005) Tidally phased emergence events in a strongly tidal estuary. Estuaries 28:500–509

Theroux RB, Wigley RL (1998) Quantitative composition and distribution of the macrobenthic invertebrate fauna of the continental shelf ecosystems of the northeastern United States. NOAA Tech Rep NMFS 140:1–240

Tiews K (1970) Synopsis of biological data on the common shrimp *Crangon crangon* (Linnaeus, 1758). FAO Fish Rep 4:1167–1224

Werner FE, Page FH, Lynch DR, Loder JW and others (1993) Influences of mean advection and simple behavior on the distribution of cod and haddock early life stages on Georges Bank. Fish Oceanogr 2:43–64

Werner FE, Perry RI, Lough RG, Naimie CE (1996) Trophodynamic and advective influences on Georges Bank larval cod and haddock. Deep-Sea Res II 43:1793–1822

Whitely GC Jr (1948) The distribution of larger planktonic crustacean on Georges Bank. Ecol Monogr 18:234–264

Wiebe PH, Morton AW, Bradley AM, Backus RH and others (1985) New developments in the MOCNESS, an apparatus for sampling zooplankton and micronekton. Mar Biol 87:313–323

Wigley RL, Burns BR (1971) Distribution and biology of mysids (Crustacea, Mysidacea) from the Atlantic coast of the United States in the NMFS Woods Hole collection. Fish Bull 69:717–746

Williams AB, Bowman RE, Damkaer DM (1974) Distribution, variation and supplemental description of the opossum shrimp, *Neomysis americana* (Crustacea: Mysidacea). Fish Bull 72:835–842

Winterwerp JC, van Kesteren WGM (2004) Introduction to the physics of cohesive sediment in the marine environment. Elsevier, New York, NY

Editorial responsibility: Alejandro Gallego, Aberdeen, UK

Submitted: October 29, 2013; Accepted: July 30, 2014
Proofs received from author(s): October 20, 2014